JOURNAL OF MATERIALS SCIENCE **34** (1999) 4489–4500

Effect of crystalline phase, orientation and temperature on the dielectric properties of poly (vinylidene fluoride) (PVDF)

R. GREGORIO, JR.*
Department of Materials Engineering, Federal University of São Carlos, C.P. 676, CEP 13.565-905, São Carlos, São Paulo, Brazil
E-mail: gregorio@power.ufscar.br

E. M. UENO
Department of Materials Engineering, State University of Ponta Grossa, CEP 84031-510, Ponta Grossa-Paraná, Brazil

The effect of crystalline phase, uniaxial drawing and temperature on the real (ε') and imaginary (ε'') parts of the relative complex permittivity of poly (vinylidene fluoride) (PVDF) was studied in the frequency range between 10^2 and 10^6 Hz. Samples containing predominantly α and β phases, or a mixture of these, were obtained by crystallization from a DMF solution at different temperatures. α phase samples were also obtained from melt crystallization and from commercial films supplied by Bemberg Folien. Different molecular orientations were obtained by uniaxial drawing of α and β phase samples. The results showed that the crystalline phase exerts strong influence on the values of ε' and ε'', indicating that the α_a relaxation process, associated with the glass transition of PVDF, is not exclusively related to the amorphous region of the polymer. An interphase region, which maintains the conformational characteristics of the crystalline regions, should influence the process decisively. The molecular orientation increased the values of ε' for both PVDF phases and modified its dependence with temperature over the whole frequency range studied. The influence of the crystallization and molecular orientation conditions on the dc electric conductivity (σ_{dc}) were also verified. The value of σ_{dc} was slightly higher for samples crystallized from solution at the lowest temperature and decreased with draw ratio.

1. Introduction

Piezoelectric polymers are intrinsically superior to piezoelectric ceramics in applications where an acoustic impedance similar to that of water or living tissue of the transducer material is required. This is the case of ultrasonic transducers for devices used in biomedical applications, which on using polymers present a better response gain, besides the high image resolution. For this reason pyro and piezoelectric polymers, like poly (vinylidene fluoride) (PVDF) and copolymers of vinylidene fluoride (VDF) and trifluorethylene (TrFE), are increasingly used as electrothermal and electromechanical transducer materials, with promising medical and industrial applications [1–6]. However, technological improvement of such devices depends on the processing techniques of the films of which the desirable properties are optimized, uniform and reproducible, and that present high thermal stability. This requires a better understanding of the influence of the crystalline phase, morphology and orientation caused by mechanical drawing on the dielectric relaxation processes that occur in these materials and which, in last analysis, account for the pyro and piezoelectric properties that they might present. PVDF is a semicrystalline polymer that besides its pyro and piezoelectric properties also possess high elasticity and is easy to process in the form of films. Its high permittivity, relatively low dissipation factor and high dielectric strength have made this polymer also very useful as capacitor dielectric. The great diversity in dielectric behavior presented by this polymer is partly due to its polymorphism, enabling crystallization into at least four phases, known as α, β, γ and δ (or II, I, III and VI, respectively). The apolar α phase is the most common, being normally obtained by melt crystallization at temperatures below 160 °C. Temperatures above this value produce a mixture of α and γ phases, being that the γ fraction increases with crystallization temperature and time [7]. However, the phase that has aroused more technological interest, for providing the best pyro and piezoelectrical properties,

* Author to whom all correspondence should be addressed.

is the β phase. This phase may be obtained by mechanical drawing of originally α phase films. Conversion of the α into the β phase, whose efficiency increases with draw ratio, only takes place when drawing is realized at temperatures lower than 100 °C. Higher temperatures reduce the content of α phase transformed into β, being that above 120 °C practically no conversion occurs, resulting in the oriented α phase [8]. Conversion into the β phase at high temperature only takes place for draw ratios above 5 [9]. Obtaining films in the β phase through drawing has hampered investigations regarding the influence of the crystalline phase on the mechanical and dielectric relaxation processes that occur in PVDF, as well as on its dielectric and piezoelectric properties, because of the additional variable drawing brings about. Recent works [7, 10] have shown that crystallization of PVDF from solution with dimethylformamide (DMF) or dimethylacetamide (DMA), may result in the α or β phases or still in a mixture of these phases. Predominance of one of these is determined by the temperature at which solvent evaporation occurs. Temperatures lower than 70 °C produce films exclusively in the polar β phase, between 70 and 110 °C a mixture of the α and β phases and above 110 °C predominantly the α phase. It has also been demonstrated that drawing of β phase films obtained by solution casting always result in this oriented phase, regardless of the process temperature [11]. In this way it is possible to obtain films in the α and β phase, or with different proportions of these phases, without orientation and oriented at different draw ratios and to verify, separately, the influence of the crystalline phase and of drawing on the relaxation processes that may occur in PVDF, as well as on its dielectric and piezoelectric properties.

The scope of this work was to investigate the effect of the crystalline phase, draw ratio and temperature on the real and imaginary parts of the relative complex permittivity in the frequency range between 10^2 and 10^6 Hz and on the dc conductivity of PVDF.

2. Experimental

2.1. Sample preparation

Films with thickness around 10 μm were obtained by spreading a solution of PVDF (FORAFLON F4000-Atochem) in DMF on a glass slide. The initial concentration of the solution was 30%. The system was maintained on a hot plate, with temperature control, for 60 min inside a closed system with exhaustion. This time was sufficient for solvent evaporation and isothermal crystallization of the PVDF. Films crystallized at 60 °C presented predominantly the β phase (PVDF-β), at 90 °C a mixture of the α and β phases and at 120 °C the α phase (PVDF-α). In order to guarantee removal of residual solvent, all samples were subsequently maintained at 120 °C for 10 h inside a muffle. This treatment practically did not alter the phase, or phases, present in the samples. Films of PVDF-α were also obtained by melting solution cast films. These were maintained at 220 °C for 10 min and subsequently quickly cooled to room temperature.

The PVDF-β films showed to be porous and to have low mechanical strength, probably due to the low temperature at which crystallization took place (60 °C). This made drawing of these films difficult and, therefore, oriented β phase films were obtained by uniaxial drawing of films crystallized from solution at 75 °C, which presented predominantly the β phase with a small amount of the α phase. These films were more resistant and could be easily drawn. These films and the PVDF-α ones obtained from rapid cooling of the melted films, were uniaxially drawn at 140 °C with draw ratios ($R =$ ratio between the final and initial length of the film) of 3 and 4, resulting in the β and α phase, respectively, with different degrees of orientation. For comparison sake unoriented PVDF-α film samples, commercially produced by Bemberg-Folien GmbH, were also used as received and drawn with $R = 3$ and 4. Drawing at 75 °C resulted in films oriented predominantly in the β phase and at 140 °C in the α phase. The crystalline phase (or phases) present in each sample was confirmed by infrared spectroscopy (Carl Zeiss) and X-ray diffractometry (Rigaku Rotaflex RU-200B with copper filter). The values of heat enthalpy (ΔH), proportional to the degree of crystallinity of each sample, were determined by differential scanning calorimetry (DSC-Du Pont, Mod. V4.OB2000), using a heating rate of 10 °C/min. Electronic micrographs were obtained by a Hitashi Mod. S-4500 microscope with acceleration voltage between 1 and 2 kV.

2.2. Electrical measurements

The real (ε') and imaginary (ε'') parts of the relative complex permittivity ($\varepsilon^* = \varepsilon' - j\varepsilon''$) were determined from the values of the capacitance and phase angle measured by a complex impedance analyzer (Mod. LF 4192A from HP) in the frequency range from 10^2 to 10^6 Hz with temperature varying between 30 and 90 °C and ambient atmosphere (relative humidity around 75%). The conduction current (I) as a function of the intensity of the applied electric field (E) was measured using an electrometer (Keithly Mod. 610C) and a stabilized voltage supply (Keithly Mod. 247). The value of I was obtained after 60 min of E application, the time necessary to reduce the strong transient current (absorption current) that arises soon after the field is applied. The E intensity varied from 1.0 to 20 MV/m. Aluminum electrodes with area of 1 cm^2 were vacuum evaporated on both sides of the samples. Before each measurement the samples were kept for 24 h in a desiccator containing silica gel in order to reduce possible effects of adsorbed moisture. The current measurements were performed at room temperature (25 °C) and 75% rh.

3. Results and discussion

3.1. Sample characterization

Fig. 1 illustrates the infrared (IR) spectra of the samples crystallized from solution at different temperatures. From the characteristic absorption bands of the β (511 and 840 cm^{-1}) and α phase (408, 531, 612, 765, 796,

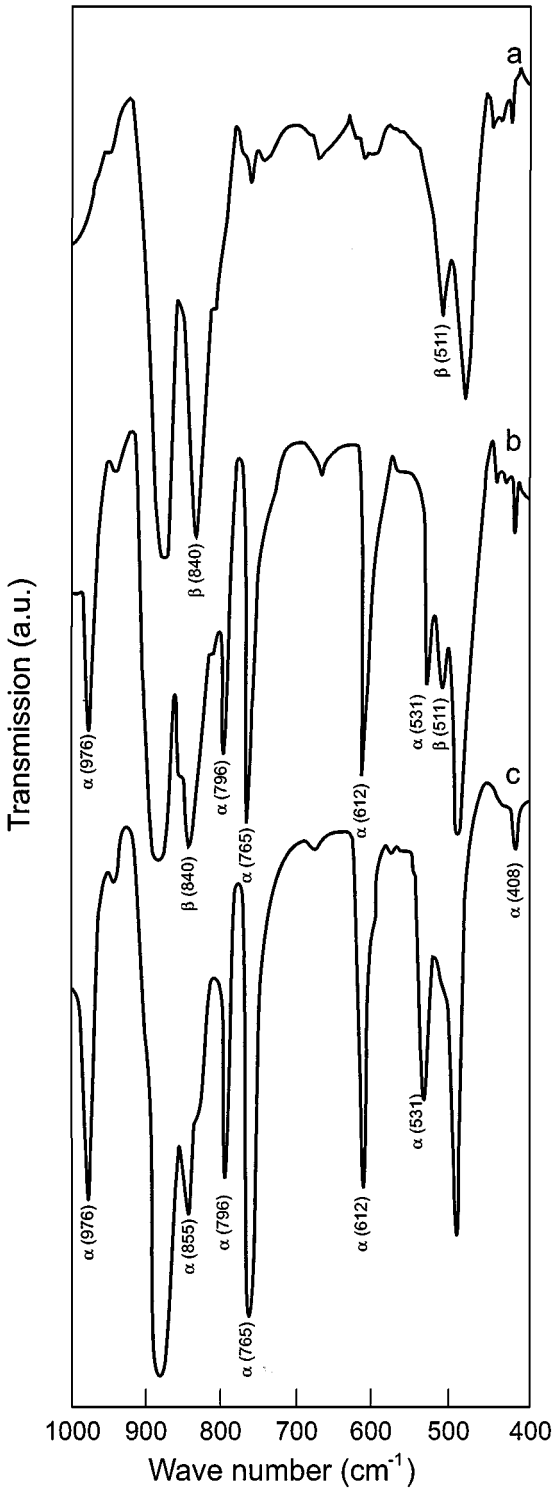

Figure 1 IR spectra of the samples crystallized from solution at: (a) 60, (b) 90 and (c) 120 °C. The characteristic absorption bands of the α and β phases are indicated in the figure.

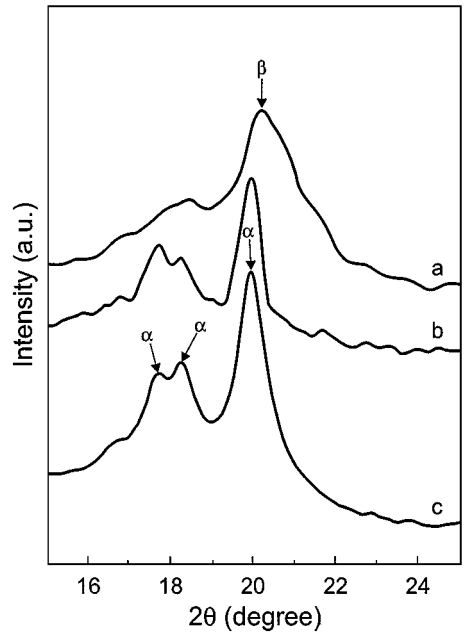

Figure 2 X-ray diffractograms of the samples crystallized from solution at: (a) 60, (b) 90 and (c) 120 °C. The arrows indicate the characteristic peaks of the α and β phases.

855 and 976 cm^{-1}) a complete predominance can be seen of the β phase in the sample crystallized at 60 °C, of the α phase in the one crystallized at 120 °C and the coexistence of both phases in that crystallized at 90 °C. These results, in agreement with those obtained in previous works [7, 10], were confirmed by X-ray diffractometry, as shown in Fig. 2. The peak at $2\theta \cong 20.3°$ refers to the sum of the diffraction in the (110) and (200) planes, characteristic of the β phase. The peaks at $2\theta \cong 17.7$, 18.4 and 19.9° refer to the diffractions in the (100), (020) and (021) planes, respectively, all characteristic of the α phase. Figs 3 and 4 show the IR spectra of the PVDF-α, crystallized from the melt and the PVDF-β samples, crystallized from solution at 75 °C, respectively, before and after drawing at 140 °C with ratios of 3 and 4. As expected, drawing of PVDF-α films realized at this temperature practically did not cause phase conversion, only orientation of the original phase. However, as can be seen in Fig. 3 the 840 cm^{-1} band becomes a little more intense, indicating a small increase in the β phase with drawing. This increase is also confirmed by the appearance of the 420 and 472 cm^{-1} band, characteristic of the oriented β phase. On the other hand, the PVDF-β film crystallized at 75 °C containing predominantly the β phase with a small amount of the α phase became almost exclusively the β phase after drawing. It is also interesting to note the appearance of the bands at 420 and 472 cm^{-1}, characteristic of the β phase in oriented films. Again the results were confirmed by X-ray diffractometry, as shown in Figs 5 and 6. Figs 7 and 8 show the IR spectra of the samples supplied by Bemberg, before and after drawing at 75 and 140 °C, respectively. Drawing at 75 °C resulted in the conversion of the α into the β phase, however with still a small amount of the α phase, evidenced by the absorptions at 612, 765 and 976 cm^{-1}, present even after drawing at a ratio of 4 (Fig. 7c). In this case the 420 and 472 cm^{-1} band, characteristic of the β phase obtained by drawing, could also be observed. Drawing at 140 °C yielded a result very similar to that obtained with the PVDF-α sample obtained by fusion (Fig. 3), i.e., predominance of the oriented α phase with a small amount of the β phase, evidenced by the bands at 420, 472 and 840 cm^{-1}. X-ray diffraction of the Bemberg samples drawn at 75 and 140 °C are presented in Figs 9 and 10, respectively. Table I lists the preparation techniques, predominant crystalline phase and the enthalpy of fusion (ΔH) of the samples investigated.

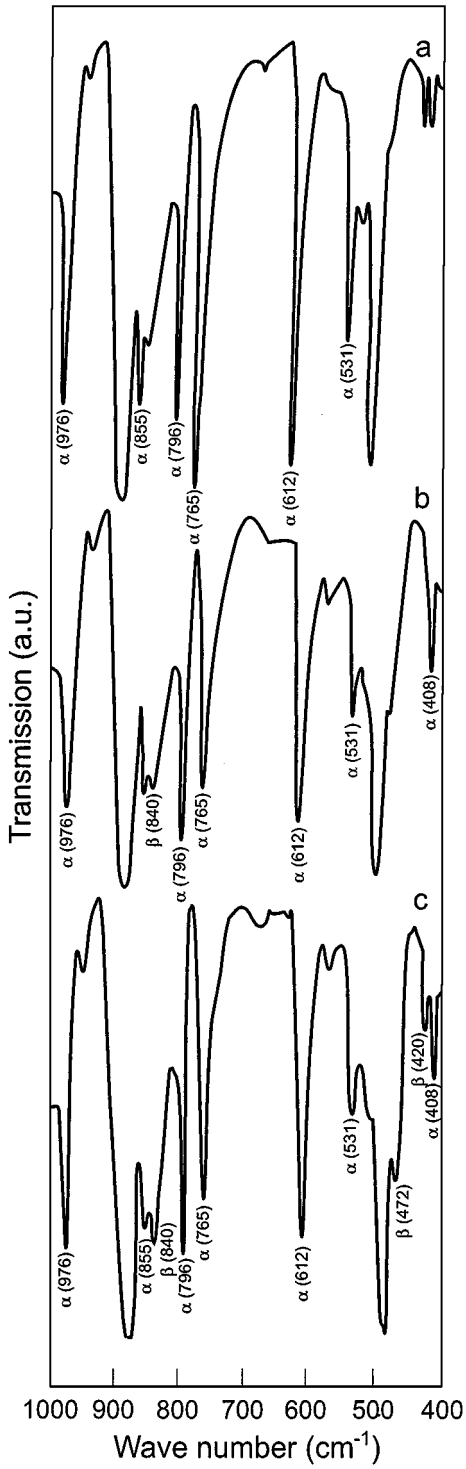

Figure 3 IR spectra of the PVDF-α sample crystallized from the melt, before (a) and after drawing at 140 °C with $R = 3$ (b) and $R = 4$ (c).

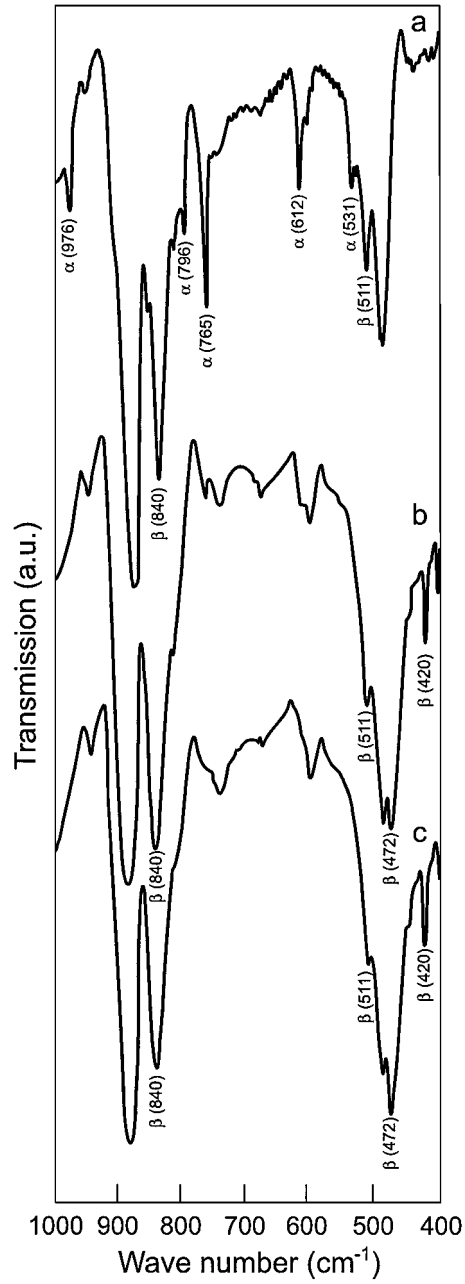

Figure 4 IR spectra of the PVDF-β sample crystallized from solution at 75 °C, before (a) and after drawing at 140 °C with $R = 3$ (b) and $R = 4$ (c).

3.2. Electric measurements

3.2.1. Real and imaginary parts of the complex relative permittivity

Fig. 11 illustrates the variation in ε' and ε'' with frequency, at room temperature, for the samples crystallized from solution at different temperatures, i.e., with different proportions of the α and β phases (samples A, B and C). The increase in ε'' with frequency, observed in the high frequency regions ($f > 10^4$ Hz) is attributed to the α_a relaxation process (also named β relaxation by some authors), associated with the glass transition of PVDF. The origin of this relaxation has caused some controversy. Some authors attribute this process to the micro-Brownian movement of the amorphous phase chain segments [12–15] (this is, above the glass transition temperature, T_g, the molecules of this phase acquire sufficient mobility for the dipoles to orient under the action of an electric field), and others to the movement of crystalline-amorphous interphase chain segments, where transition takes place of the perfect crystalline order to the isotropy of the amorphous state [16, 17]. This dipolar relaxation process, that accounts for the high value of ε' of PVDF, presents a maximum of ε'' close to 2 MHz at 20 °C [13, 14, 18], therefore not observed in our experiments. In the low frequency range ($f < 10^3$ Hz) the small increase in ε' and the strong increase in ε'' with the decrease in frequency probably occurs due to the ionic dc conduction contribution, which results in interfacial or spatial

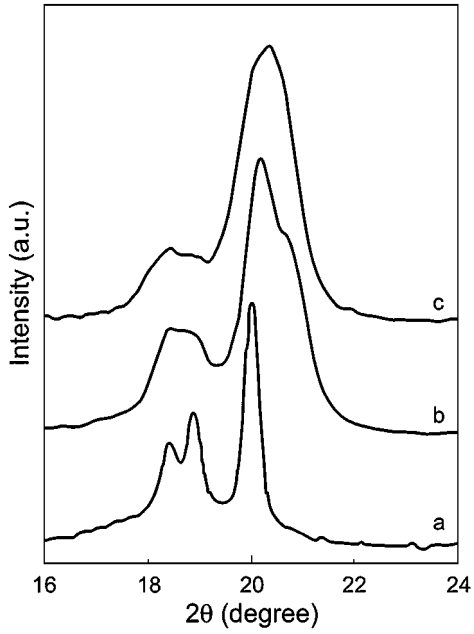

Figure 5 X-ray diffractograms of the sample crystallized from the melt, before (a) and after drawing at 140 °C with $R = 3$ (b) and $R = 4$ (c).

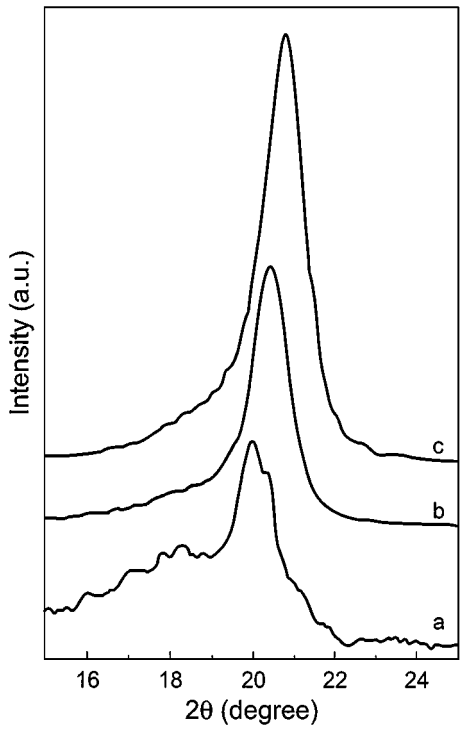

Figure 6 X-ray diffractograms of the sample crystallized from solution at 75 °C, before (a) and after drawing at 140 °C with $R = 3$ (b) and $R = 4$ (c).

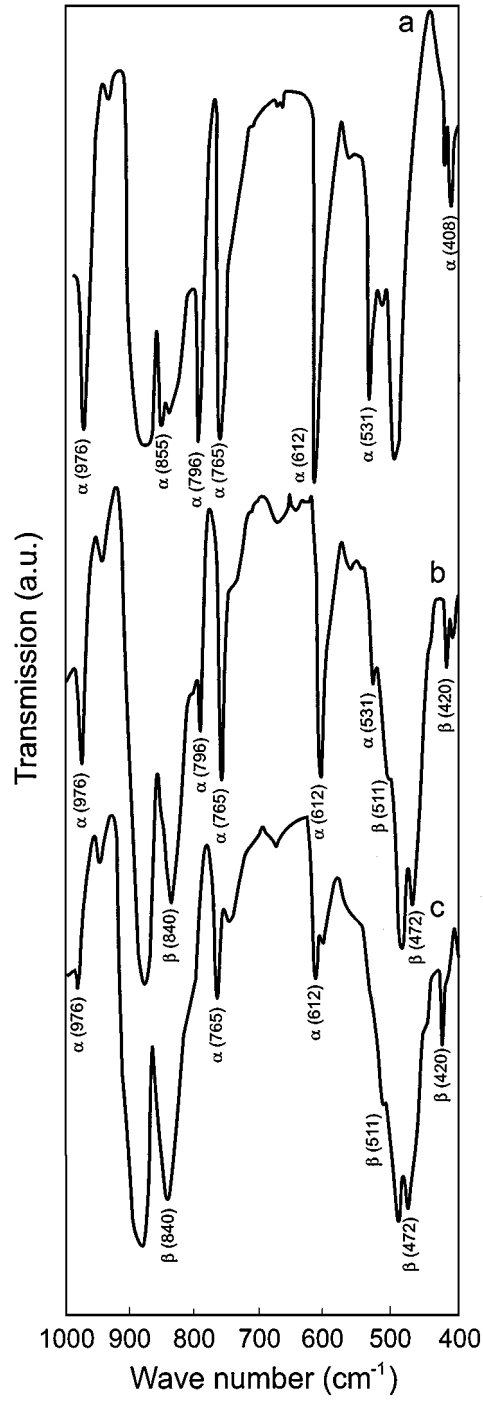

Figure 7 IR spectra of the sample supplied by Bemberg, before (a) and after drawing at 75 °C with $R = 3$ (b) and $R = 4$ (c).

charge polarization, since the α_c relaxation, related to the molecular movement of the polymer chains in the crystalline region due to orientation of the dipoles, is less likely to happen at room temperature with the low intensity of the electric field applied.

In the whole frequency range analyzed ε' is seen to increase with the amount of β phase present in the sample. Since the percentage of the amorphous phase of the three samples should not differ much, as they possess very similar ΔH values (Table I), these results suggest that the α_a relaxation process is not exclusively related to the amorphous PVDF phase. The strong effect of the crystalline phase on the ε' values here observed leads us to assume that this relaxation is likely related mainly to the cooperative orientational movement of the existing dipoles in the crystalline-amorphous interphase of PVDF, as suggested by Hahn and coworkers [16] and by Ando and coworkers [17]. This interphase maintains the characteristics of the molecular order of the crystalline region, and therefore of the molecular structure of the predominant molecular form, without presenting the mobility restraints of the rigid network. The difference among the values of ε' observed for samples A, B and C (Fig. 11) is probably related to the different

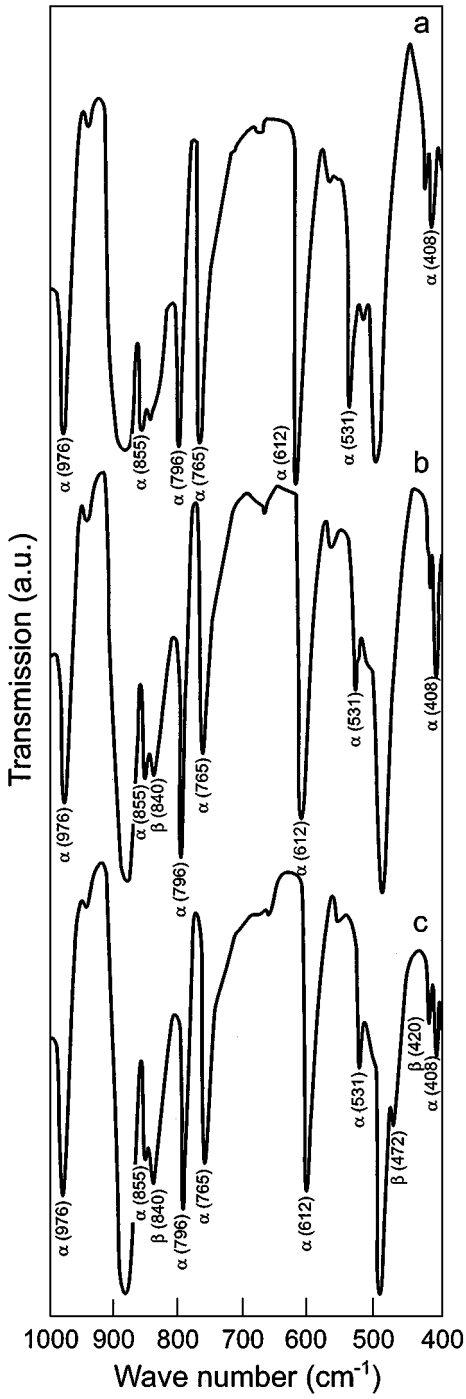

Figure 8 IR spectra of the sample supplied by Bemberg, before (a) and after drawing at 140 °C with $R = 3$ (b) and $R = 4$ (c).

TABLE I Preparation techniques, predominant crystalline phase and enthalpy of fusion of the investigated samples

Sample	Preparation techniques	Predominant crystalline phase	ΔH (J/g)
A	From solution at 60 °C	β	56
B	From solution at 90 °C	α e β	58
C	From solution at 120 °C	α	60
D	From solution at 75 °C	β	58
E	D drawn at 140 °C and $R = 3$	β oriented	60
F	D drawn at 140 °C and $R = 4$	β oriented	65
G	From the melt	α	58
H	G drawn at 140 °C and $R = 3$	α oriented	60
I	G drawn at 140 °C and $R = 4$	α oriented	62
J	As received from Bemberg	α	52
K	J drawn at 75 °C and $R = 3$	β oriented	55
L	J drawn at 75 °C and $R = 4$	β oriented	57
M	J drawn at 140 °C and $R = 3$	α oriented	57
N	J drawn at 140 °C and $R = 4$	α oriented	59

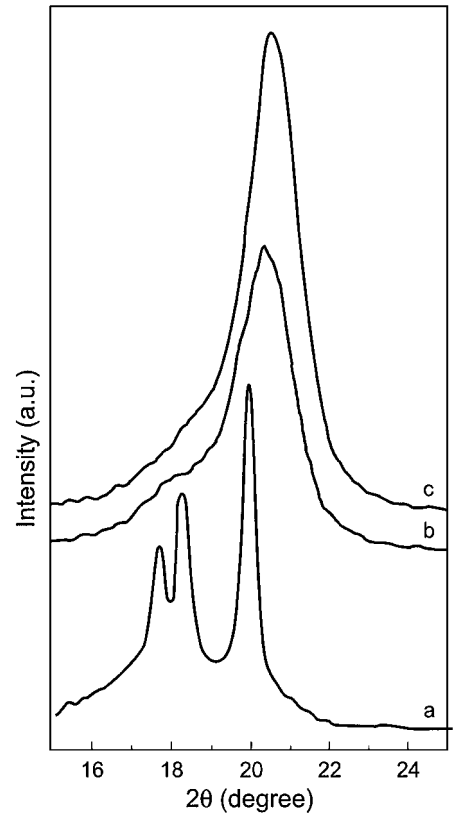

Figure 9 X-ray diffractograms of the sample supplied by Bemberg, before (a) and after drawing at 75 °C with $R = 3$ (b) and $R = 4$ (c).

characteristics of these interphases such as molecular order and thickness. The sample crystallized at lower temperature should have thicker interphases (the ratio between the percentage interphase and that of the amorphous region is higher) maintaining the molecular order characteristics of the β phase, in this way resulting in larger polarization. With increase in crystallization temperature the thickness of the interphase is supposed to decrease and the molecular order to become more similar to that of the apolar α phase, reducing the value of ε'. The difference in morphology presented by these three samples might also be interfering in the polarization process. A recent work [19] has shown that samples crystallized from solution at 60 °C present very small spherulites, with average diameter in the order of 5 μm, and high porosity. Fibrils, highly oriented due to the action of tension forces during the solidification process, were also seen to come into existence between these spherulites. With increase in crystallization temperature the spherulites become larger and porosity diminishes. Fig. 12a and b show micrographs obtained by low voltage scanning electron microscopy of the spherulite morphology presented by the samples crystallized at 60 °C (sample A) and at 120 °C (sample C), respectively. Fig. 13 shows an amplified detail of the morphology presented in Fig. 12a, where the highly oriented fibrils between two spherulites can be seen. The sample crystallized at 120 °C (Fig. 12b) is

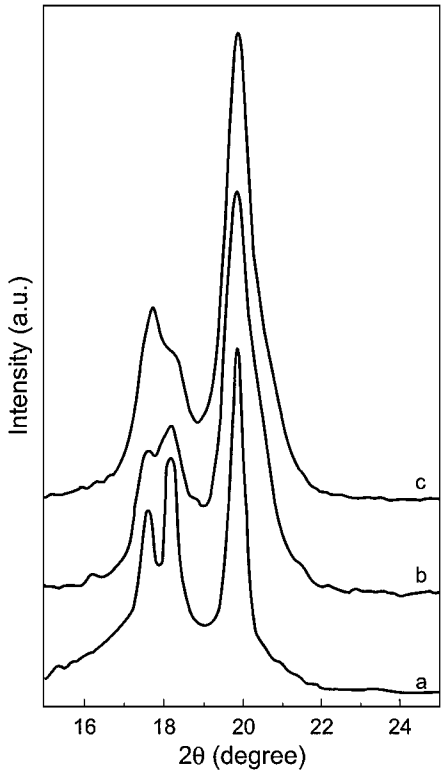

Figure 10 X-ray diffractograms of the sample supplied by Bemberg, before (a) and after drawing at 140 °C with $R = 3$ (b) and $R = 4$ (c).

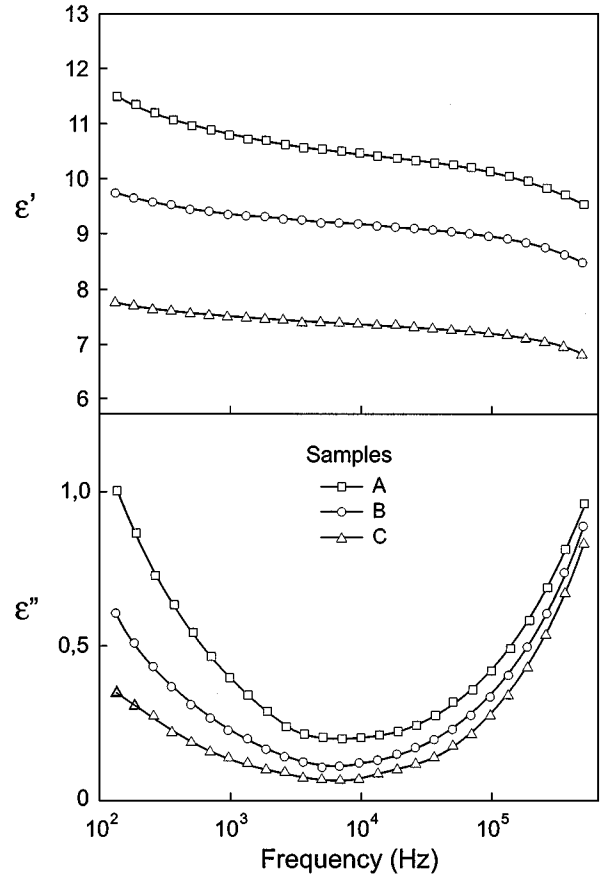

Figure 11 Variation in ε' and ε'' with frequency for the samples crystallized from solution at: 60 (□), 90 (○) and 120 °C (Δ).

seen to be less porous, to have larger spherulites (average diameter 8 μm) and to lack the oriented fibrils between the spherulites. The different morphologies presented by samples A, B and C may also be affecting the orientation of the dipoles existing at the interphases of PVDF, resulting in different ε' values. Indeed, in semicrystalline polymers that crystallize as spherulites the amorphous and crystalline regions are so intimately interlinked that it is not possible to separate them into distinct regions. Almost the whole amorphous region may be considered an interphase region that maintains a conformation strongly influenced by the crystalline region. A study on the effect of the morphology, crystalline phase and drawing on the α_a and α_c relaxation processes of PVDF is being carried out by means of dielectric measurements in a wider range of frequency (10^{-2} to 10^7 Hz) and temperature (-60 to 150 °C), and the results may give some insight into the role performed by the amorphous and crystalline phases and by the interphases in these processes.

The effect of uniaxial orientation at 140 °C on the variation in ε' and ε'' with frequency, at room temperature, of samples D (PVDF-β) and G (PVDF-α) can be seen in Figs 14 and 15, respectively. As seen, drawing at this temperature does not cause phase conversion only orientation of the original phase. In both cases ε' is seen to increase with draw ratio. Drawing destroys the spherulitic morphology, characteristic of PVDF, and aligns the chains preferentially in the stress direction, parallel to the film surface, facilitating orientation of the components of the dipole moments normal to these chains by the electric field, applied normal to this surface. Moreover, higher chain packing caused by drawing might be increasing the dipole density, which would also contribute to the increase in ε'. The results also show that drawing affects ε' more strongly for sample in the α phase than for sample in the β phase. One may also note that of the undrawn samples containing predominantly the α phase (C and G), the one obtained through crystallization from solution at 120 °C presented ε' values slightly lower than those obtained from rapid cooling of the melt (compare Figs 11(Δ) and 15(□)). This result might be related to the difference in porosity between these samples. Normally, samples obtained from solution are more porous than those obtained from the melt, and this results in different dipole densities. Another probable cause would be the difference in morphology that these samples present and which is related to their thermal history.

Figs 16 and 17 present the variation in ε' and ε'' with frequency, at room temperature, for the sample commercially produced by Bemberg (J), before and after drawing at 75 and 140 °C, respectively. Sample J presented values of ε' slightly higher than those obtained for sample G (compare Figs 15(□) and 16(□)), despite the fact that both present predominantly the unoriented α phase. This difference has likely occurred due to the different processing of the samples. Sample J was obtained by blowing, which results in partially bioriented films. However, a more noteworthy difference occurred between these samples after drawing. The increase in ε' with drawing realized at 140 °C was more intense for sample G (Fig. 15(○)) than for sample J (Fig. 17(○)), for a draw ratio of 3. It is interesting to note as well that drawing at a ratio of 4 of sample J at 75 °C (Fig. 16(Δ)),

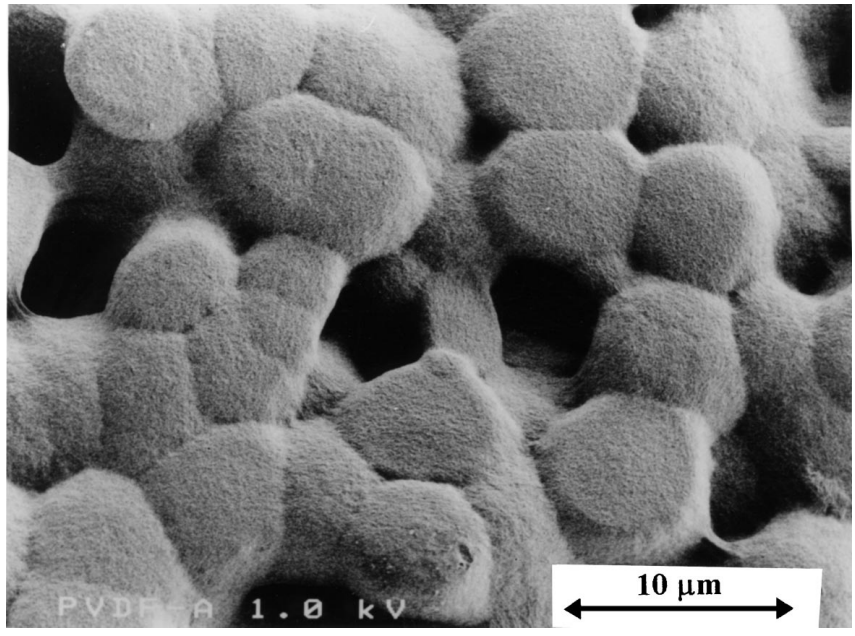

(a)

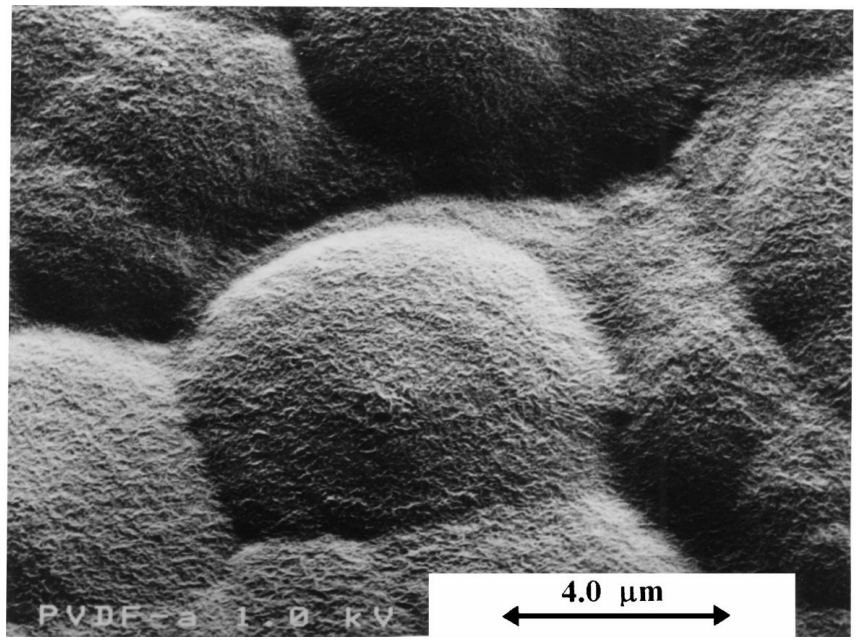

(b)

Figure 12 Micrographs obtained by SEM for samples crystallized from solution at: (a) 60 and (b) 120 °C.

and which resulted in the transition of the α into the β phase besides the orientation, provided values of ε' slightly lower than those obtained with the same draw ratio at 140 °C (Fig. 17(Δ)), where this transition did not take place.

Figs 18 and 19 illustrate the variation in ε' and ε'' with frequency for temperatures varying from 30 to 90 °C for samples G and I, respectively, i.e., for PVDF-α unoriented and oriented at 140 °C with a ratio of 4. The unoriented sample (G) shows a strong increase in ε' and ε'' with temperature in the low frequency range ($f < 10^4$ Hz). This increase likely occurs due to the superposition of two effects: the increase in intensity and the shift towards higher frequencies of the maximum of ε'' related to the α_c relaxation (more likely to occur at temperatures above 50 °C), and the increase in dc conduction with consequent increase in interfacial polarization. The values of ε' and ε'' for $f > 10^4$ Hz, where dipolar polarization that occurs in the amorphous region or interphase predominates, were in this case little affected by the temperature. The strongest effect occurs at $f > 10^5$ Hz due to the shift towards higher frequencies of the maximum of ε'' with temperature increase. After drawing (samples I), besides their increase, as already observed, the values of ε' become more sensitive to the variation in temperature at high frequencies ($f > 10^4$ Hz). On the contrary, the strong increase in ε' and ε'' with temperature, verified before drawing at low frequencies ($f < 10^4$ Hz) became less intense, indicating a probable reduction in dc

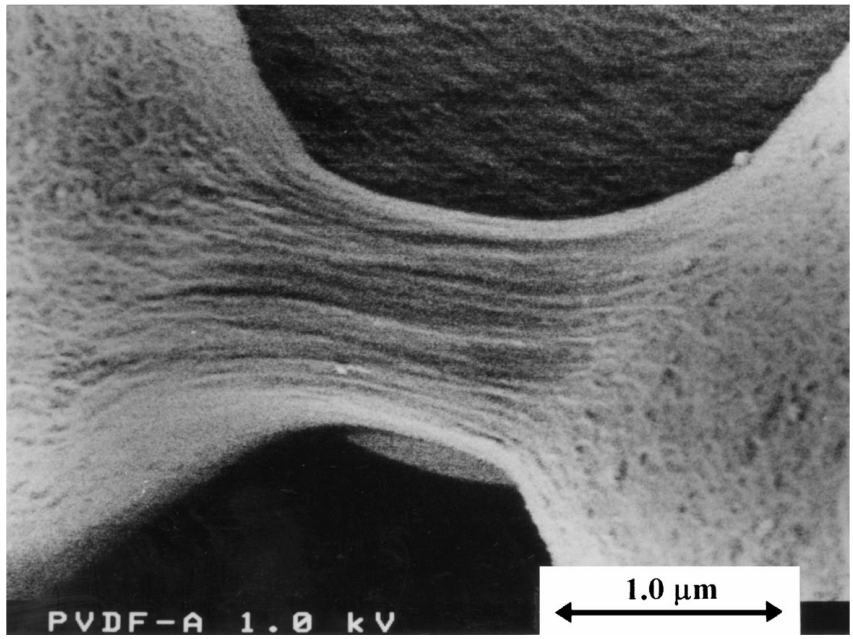

Figure 13 Detail of the morphology presented by the sample crystallized at 60 °C (the same as Fig. 12a), showing oriented fibrils between two spherulites.

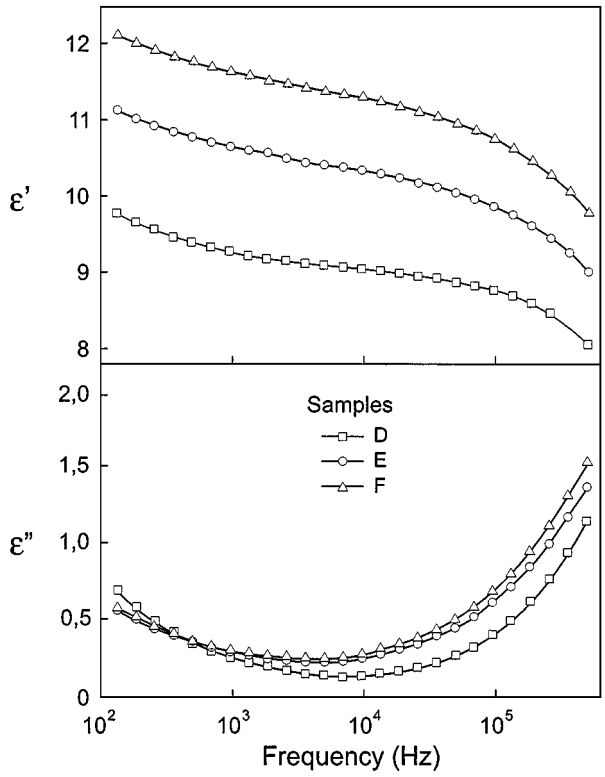

Figure 14 Variation in ε' and ε'' with frequency for a sample crystallized from solution at 75 °C, before (□), and after drawing at 140 °C with $R =$ 3 (○) and $R = 4$ (Δ).

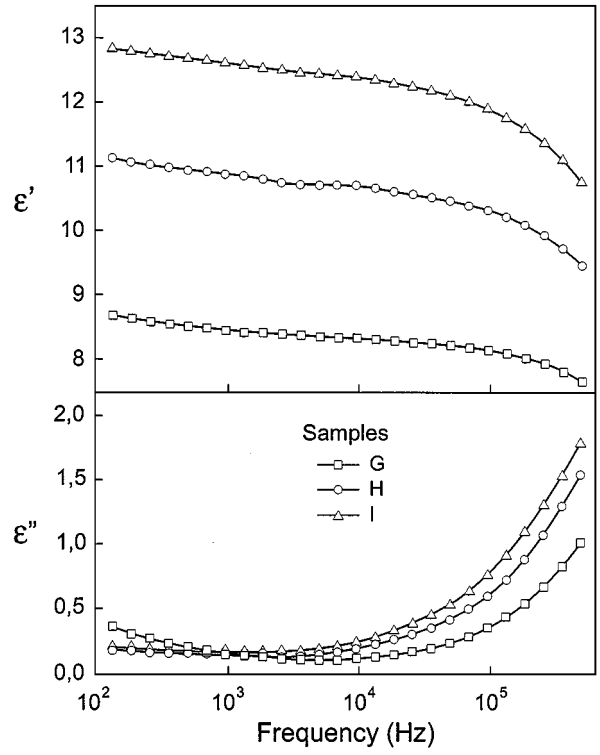

Figure 15 Variation in ε' and ε'' with frequency for a sample crystallized from melt, before (□), and after drawing at 140 °C with $R = 3$ (○) and $R = 4$ (Δ).

conductivity, and consequently, in interfacial polarization and possibly in the α_c relaxation with drawing. In the high frequency range ($f > 10^5$ Hz) a temperature increase is also seen to shift the ε'' peak, related to the α_a relaxation, towards higher frequencies. A probable reason for the stronger dependence of ε' with temperature at $f > 10^4$ Hz after drawing is the higher packing of the polymer chains when oriented. As the T_g of PVDF is very low ($\cong -36$ °C) [10] in the unoriented sample orientation of the dipoles in the amorphous region or interphase is little affected by the temperature in the range between 30 and 90 °C, because the mobility of the chains is little altered in this temperature range. With drawing the higher chain packing causes an increase in dipole density, which collaborates with the increase in ε', however it restrains chain mobility, hampering the orientation process of their dipoles. The temperature increase reduces the tension on the molecules caused

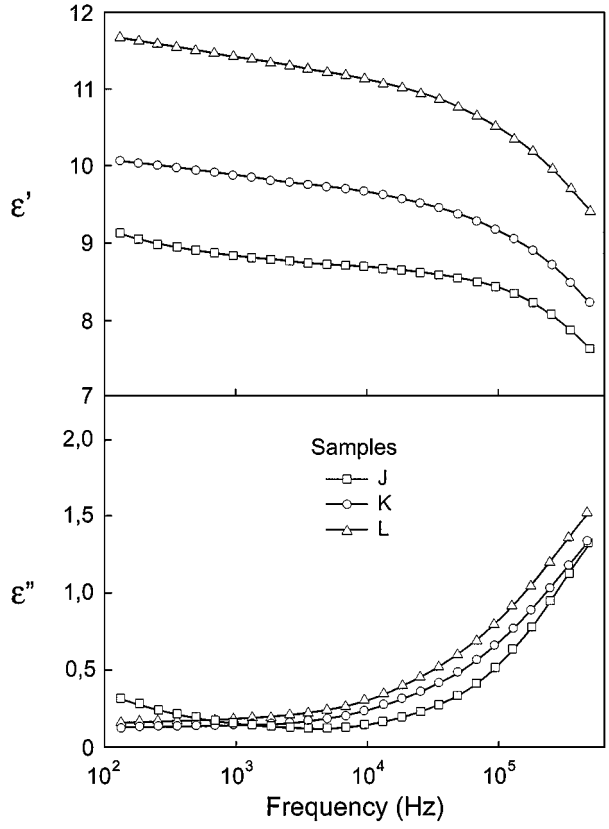

Figure 16 Variation in ε' and ε'' with frequency for a sample supplied by Bemberg, before (□) and after drawing at 75 °C with $R = 3$ (○) and $R = 4$ (Δ).

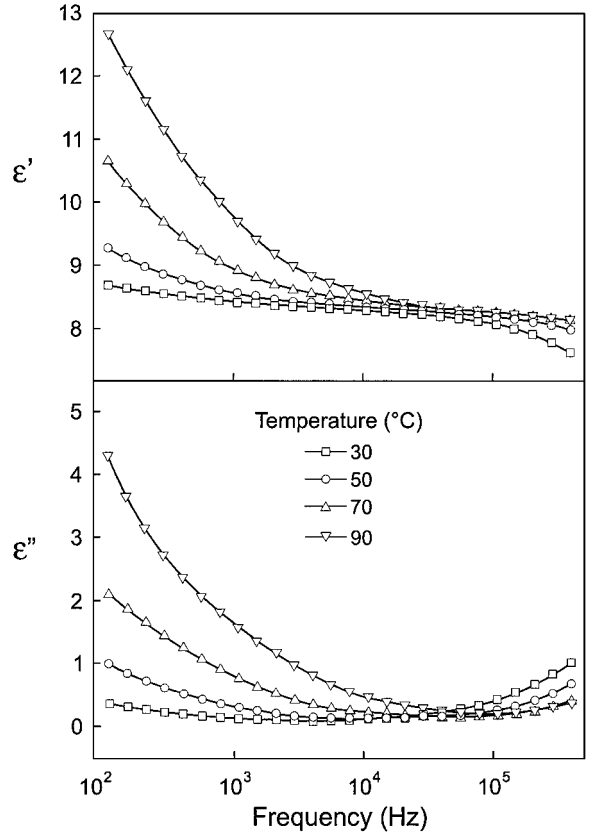

Figure 18 Variation in ε' and ε'' with frequency at different temperatures for a sample crystallized from the melt.

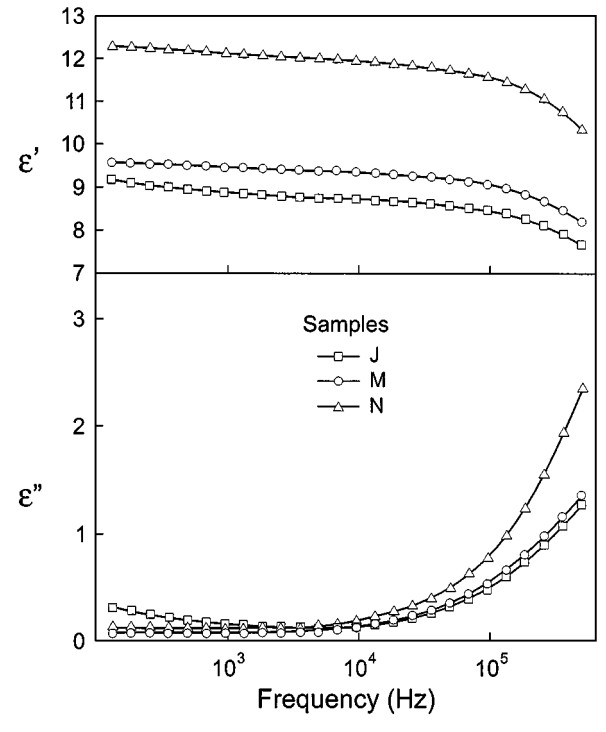

Figure 17 Variation in ε' and ε'' with frequency for sample supplied by Bemberg, before (□), and after drawing at 140 °C with $R = 3$ (○) and $R = 4$ (Δ).

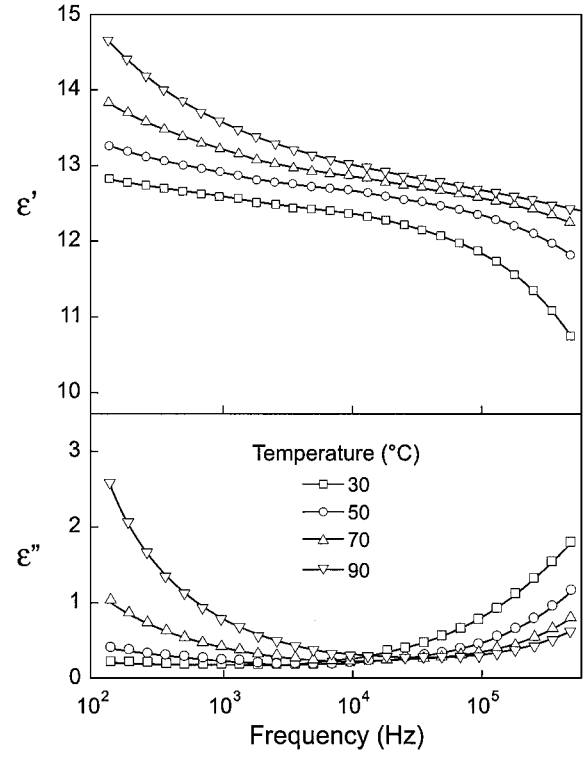

Figure 19 Variation in ε' and ε'' with frequency at different temperatures for a sample crystallized from the melt after drawing at 140 °C with $R = 4$.

by drawing (relaxation), reducing packing and making the dipoles freer to orient. This increases the dipolar orientation and, consequently, the values of ε'. The values of ε'' for frequencies lower than 10^4 Hz were reduced after drawing. This behavior is to some extent likely related to the decrease in dc conductivity with drawing, as will be seen in the next item. In all samples investigated the effect of drawing on the variation in ε'

and ε'' with temperature was similar to that described for sample G.

3.2.2. DC conductivity

Fig. 20 illustrates the variation in current density (J) as a function of the intensity of the electric field applied (E), at room temperature, for sample G (PVDF-α) with different draw ratios (samples H and I). The full lines were obtained by fitting the experimental values to the expression developed by Mott and Gurney [20], a theoretical model for the ionic conduction through carrier hopping:

$$J \propto \sin h(qEd/2kT) \tag{1}$$

where q is the ion charge, d is the average distance between hoppings, k is Boltzman's constant and T the absolute temperature. For elevated values of E expression (1) becomes:

$$J \propto \exp(qEd/2kT) \tag{2}$$

For a given temperature, the curve ln J versus E results in a straight line with slope given by $qd/2kT$. For $T = 300$ K, the values of d for samples G, H and I were 5.3, 4.4 and 4.2 nm, respectively. The dc conductivity values, σ_{dc}, for $E = 1.0$ MV/m, of these three samples resulted in 2.8×10^{-11}, 1.9×10^{-11} and 1.2×10^{-11} S/m, respectively. All samples investigated presented this small reduction in the values of d and σ_{dc} with drawing. The higher chain packing caused by the drawing might have caused the reduction in d. Drawing may also have favored the formation of defects in the material that act as traps reducing the density of the carriers. As a result the drawing slightly reduced σ_{dc} of PVDF in both crystalline phases, and consequently, the values of ε' and ε'' at low frequencies, as previously noted. Fig. 21 shows the dependence of J with the intensity of the E, at room temperature, for the samples containing different amounts of α and β phases (samples A, B and C). J is seen to decrease with the increase in the amount of α phase. The values of d for these samples were 7.4, 5.9 and 5 nm, respectively.

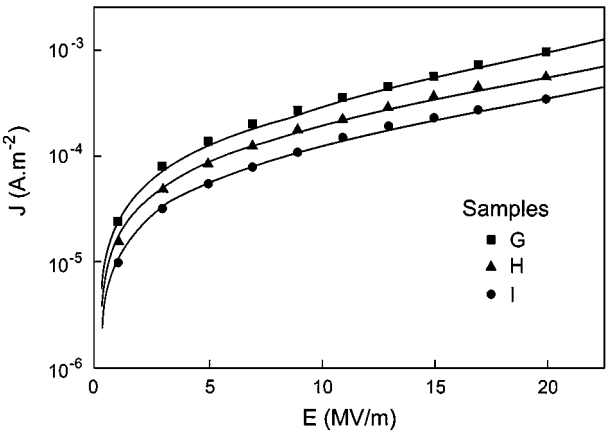

Figure 20 Conduction current density as a function of the intensity of the electric field applied for a sample crystallized from the melt, before (■) and after drawing at 140 °C with $R = 3$ (▲) and $R = 4$ (●). The full lines were obtained by fitting the experimental values to the expression developed by Mott and Gurney [20].

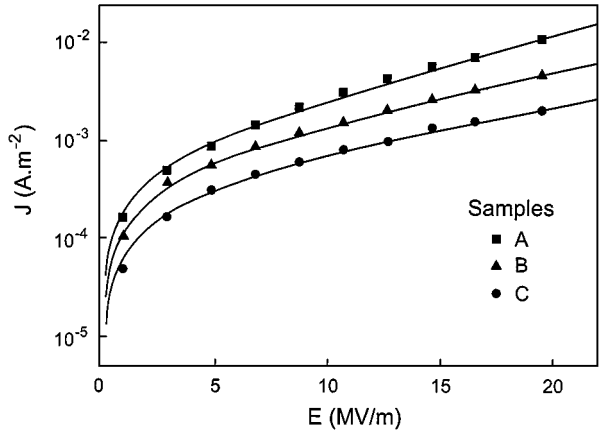

Figure 21 Conduction current density as a function of the intensity of the electric field applied for samples crystallized from solution at 60 (■), 90 (●) and 120 °C (▲). The full lines were obtained by fitting the experimental values to the expression developed by Mott and Gurney [20].

The dc conductivities were 1.9×10^{-11}, 1.2×10^{-11} and 5×10^{-11} S/m, respectively. This difference in the value of σ_{dc} is presumably not related to the different crystalline phases present in PVDF, as the ionic conduction occurs predominantly in the amorphous phase or interphase of the polymer. Since the three samples present very similar crystalline percentages it is quite probable that the highest conductivity of the PVDF-β is partly due to the higher density of carriers existing in this sample. The higher porosity of this sample compared to PVDF-α has probably permitted a higher adsorption of water, favoring the ionic dissociation in the material. The proper water molecules may have dissociated under the action of the electric field, contributing to the increase in the density of carriers (protonic conduction). The higher ionic conductivity presented by the more porous sample (crystallized at lower temperature) has probably been the cause of the higher value of ε'' of this sample observed at low frequencies (Fig. 11). This value is strongly reduced when the measurements are performed in dry atmosphere and with samples maintained in desiccators for a long time [21].

4. Conclusions

The crystalline phase (α and β) showed to exert strong influence on the real (ε') and imaginary (ε'') parts of the relative complex permittivity of PVDF in the frequency range from 10^2 to 10^6 Hz. The values of ε' and ε'' are higher for the samples containing predominantly the β phase and decrease with the increase in the amount of the α phase. Since in this frequency range dipolar polarization predominates, these results suggest that at room temperature orientation of the dipoles does not occur predominantly in the amorphous phase of the polymer, but in amorphous-crystalline interphase regions whose conformations are strongly affected by the neighboring crystalline phase. For both crystalline phases the value of ε' increased with draw ratio in the whole frequency range investigated. The molecular alignment caused by drawing also increased the dependence of ε' and ε'' with temperature between 30 and 90 °C for frequencies above 10^4 Hz where dipolar polarization

predominates. For frequencies lower than this value, where the effect of ionic conduction prevails resulting in interfacial polarization, the dependence of ε' with temperature and the values of ε'' were reduced. The dc electric conductivity was slightly reduced with crystallization temperature of the sample and with drawing. In the first case this probably happened due to the distinct porosity of the samples crystallized at different temperatures which could have resulted in different water adsorption. In the second case a probable cause was the higher molecular packing and the formation of defects caused by drawing.

Acknowledgements

The authors thank FAPESP and CNPq for the financial aid, and Dr. Joachim Loos for the electronic micrographs of the samples.

References

1. K. KOBAYASHI and T. YAMADA, *Ferroelectrics* **32** (1981) 181.
2. A. DEREGGI, *ibid.* **60** (1984) 83.
3. T. T. WANG, J. M. HERBERT and A. M. GLASS, "The Applications of Ferroelectric Polymers" (Chapman and Hall, New York, 1988).
4. S. HURMILA, H. STUBB, J. PITKANEN, K. LAHDENPERA and A. PENTTINEN, *Ferroelectrics* **115** (1991) 267.
5. H. MEIXNER, *ibid.* **115** (1991) 279.
6. Q. X. CHEN and P. A. PAYNE, *Meas. Sci. Techonol.* **6** (1995) 249.
7. R. GREGORIO, JR. and M. CESTARI, *J. Polym. Sci.:B: Polym. Phys.* **32** (1994) 857.
8. T. C. HSU and P. H. GEIL, *J. Mater. Sci.* **24** (1989) 1219.
9. J. C. MAGRATH and I. M. WARD, *Polymer* **21** (1980) 855.
10. R. GREGORIO, JR., R. CESTARI, N. C. P. S. NOCITI, J. A. MENDONÇA and A. A. LUCAS, "The Polymeric Materials Encyclupedia: Synthesis, Properties and Applications" (CRC Press, USA, 1996) p. 2286.
11. R. GREGORIO, JR. and J. A. MENDONÇA, in Proceedings of the 2nd Brazilian Polymer Congress, São Paulo, Brazil, October 1993, p. 535 (in Portuguese).
12. H. SASABE, S. SAITO, M. ASAHINA and H. KAKUTANI, *J. Polym. Sci.* **A2**(7) (1969) 1405.
13. S. J. YANO, *Polym. Sci.* **A2**(8) (1970) 1057.
14. K. NAKAGAWA and Y. ISHIDA, *J. Polym. Sci: Polym. Phys. Ed.* **11** (1973) 1503.
15. V. J. MCBRIERTY, D.C. DOUGLASS and T. A. WERBER, *ibid.* **14** (1976) 1271.
16. B. HAHN, J. WENDORFF and D. Y. YOON, *Macromol.* **18** (1985) 718.
17. Y. ANDO, T. HANADA and K. SAITOH, *J. Poly. Sci.:B:Poly. Phys.* **32** (1994) 179.
18. T. FURUKAWA, M. OHUCHI, A. CHIBA and M. DATE, *Macromol.* **17** (1984) 1384.
19. H. J. KESTENBACH, R. GREGORIO, JR., J. LOOS and J. PETERMANN, *Polímeros: Ciência e Tecnologia* **1** (January/March, 1997) 58 (in Portuguese).
20. N. F. MOTT and R. W. GURNEY, "Electroinc Processes in Ionic Crystals" (Oxford University Press, London, 1940) p. 43.
21. R. GREGORIO, JR. and M. CESTARI, in Proceedings of the. X CBECIMAT, Águas de Lindóia-SP, Brazil, December 1992, p. 262 (in Portuguese).

Received 5 August 1998
and accepted 26 March 1999